

LIME: LINK-BASED USER-ITEM INTERACTION MODELING WITH DECOUPLED XOR ATTENTION FOR EFFICIENT TEST TIME SCALING

Yunjiang Jiang*
 Meta
 jyj@meta.com
 Bi Xue
 Meta
 bixue@meta.com

Ayush Agarwal*
 Meta
 ayushaga@meta.com

Yang Liu†*
 Meta
 yangliu991@meta.com

ABSTRACT

Scaling large recommendation systems requires advancing three major frontiers: processing longer user histories, expanding candidate sets, and increasing model capacity. While promising, transformers’ computational cost scales quadratically with the user sequence length and linearly with the number of candidates. This trade-off makes it prohibitively expensive to expand candidate sets or increase sequence length at inference, despite the significant performance improvements.

We introduce **LIME**, a novel architecture that resolves this trade-off. Through two key innovations, LIME fundamentally reduces computational complexity. First, low-rank “link embeddings” enable pre-computation of attention weights by decoupling user and candidate interactions, making the inference cost nearly independent of candidate set size. Second, a linear attention mechanism, **LIME-XOR**, reduces the complexity with respect to user sequence length from quadratic ($O(N^2)$) to linear ($O(N)$).

Experiments on public and industrial datasets show LIME achieves near-parity with state-of-the-art transformers but with a $10\times$ inference speedup on large candidate sets or long sequence lengths. When tested on a major recommendation platform, LIME improved user engagement while maintaining minimal inference costs with respect to candidate set size and user history length, establishing a new paradigm for efficient and expressive recommendation systems.

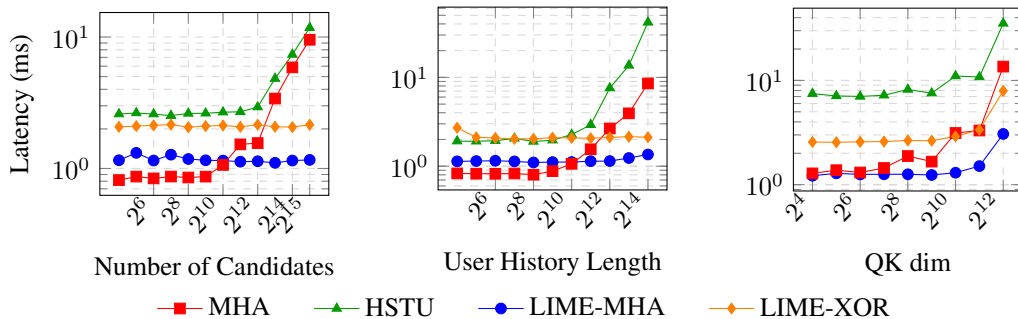


Figure 1: Overall latency analysis across different model parameters. Both LIME models scale well with history length and number of candidates to rank whereas skyline model latencies explode. Note the **logarithmic** scale in the Latency axis.

*Equal contribution.

†Corresponding author.

1 INTRODUCTION

Modern recommendation systems operate at a massive scale, facing the challenge of ranking millions of candidate items within strict real-time latency constraints. To succeed, ranking models must navigate a fundamental trade-off between computational efficiency and predictive accuracy. This has led to two dominant but conflicting architectural paradigms. On one end of the spectrum is the two-tower model (Covington et al., 2016), which achieves unparalleled inference speed by encoding users and items into separate, independent representations. This separation enables the use of efficient approximate nearest-neighbor search (Shrivastava & Li, 2014), making real-time recommendations feasible at scale.

On the other end are powerful cross-attention Transformer models like SASRec (Kang & McAuley, 2018), which deliver state-of-the-art accuracy by encoding users’ long interaction history (UIH) via multi-layer self attention and explicitly modeling deep, contextual interactions between that and each candidate item. Although this approach provides rich expressiveness, it comes with a significant computational cost: the self-attention over long sequences and the cross-attention between the full user sequence and each candidate become major performance bottlenecks. This architectural dilemma is becoming increasingly acute. The push for higher quality recommendations now demands scaling along three axes simultaneously: accommodating vast candidate sets, processing longer user histories, and deploying models of increasing complexity. These demands are fundamentally at odds, as existing efficient models lack expressiveness, while expressive models lack efficiency. Hybrid approaches (Li et al., 2022) offer only incremental improvements.

To fundamentally solve this problem and enable scaling along all three axes, we propose a new architectural blueprint: the Link-based User-Item Interaction Modeling for Efficient inference (LIME) framework. LIME is designed from the ground up to achieve the modeling power of a full cross-attention system while operating within the strict efficiency budget of a two-tower model. Its central innovation is a globally learned intermediate “link embedding” sequence that acts as a bridge between the long user history and candidate items. This design decouples the user and item representations during online inference, making scoring independent of history length by pre-computing the most expensive attention components offline. Furthermore, it enables the introduction of a new low rank attention mechanism to reduce user interaction history (UIH) self-attention complexity from quadratic to linear. By resolving these two primary computational bottlenecks, LIME provides a comprehensive solution to the expressiveness-versus-efficiency challenge, enabling deep interaction modeling at minimal latency (Figure 1).

Our primary contributions are as follows:

The Link Embedding Mechanism: We introduce a link embedding sequence that effectively approximates full cross-attention. This mechanism allows the expensive Query-Key attention weight, $\phi(\tilde{Q}\tilde{K}^\top)$, to be pre-computed and cached offline, enabling cross-attention-like expressiveness with the efficiency of Two-Tower modeling during online inference.

XOR Attention Masking: To overcome the quadratic time complexity of Transformers with respect to user history length, we propose an XOR attention mask that factorizes the full self-attention matrix into a bidirectional linear attention between the link embeddings and the user history sequence.

State-of-the-Art Performance and Impact: We demonstrate through extensive experiments that LIME achieves performance competitive with computationally intensive ranking models like HSTU (Zhai et al., 2024) with 10x lower latency. Deployed in production, LIME has yielded up to 38% source rate¹ gain on a major platform serving billions of users.

2 RELATED WORK

LIME addresses the long-standing trade-off between model expressiveness and inference efficiency in large-scale ranking. We situate our contributions in the context of two primary research areas: efficient ranking architectures and innovations in sequence modeling.

¹This refers to the percentage of positively engaged items attributable to the ranking model using LIME.

2.1 EFFICIENT RANKING ARCHITECTURES

The design of ranking models is dominated by a conflict between efficiency and interaction depth. On one end of the spectrum, two-tower models (Covington et al., 2016; Yi et al., 2019) achieve unparalleled efficiency. By encoding users and items into separate embedding spaces, they enable fast candidate retrieval using Approximate Nearest Neighbor (ANN) search. However, this separation prevents deep, feature-level interactions, limiting model expressiveness. On the other end, cross-attention models like DIN (Zhou et al., 2018) enable rich, target-aware interactions by dynamically attending to user history for each candidate, but their per-item computational cost makes them prohibitive for ranking large candidate sets.

Several approaches have sought to bridge this gap. Hybrid models add shallow interaction layers on top of a two-tower base (Li et al., 2022), though these often provide only marginal improvements. LIME offers a more fundamental solution. It introduces a novel bridge built upon a fixed set of global, learnable parameters, which we term link embeddings. These link embeddings act as an intermediary, allowing LIME to capture the rich dynamics of cross-attention while retaining the architectural efficiency of a two-tower model. This design, where a static, user-independent key space (raw links) retrieves information from a dynamic, personalized value space (personalized links), is conceptually similar to key-value memory networks (Miller, 2016) and the retrieval stage of retrieval-augmented models, enabling massive pre-computation. This approach directly tackles the sequential nature of user history and the need for scalable target-item interaction, striking a new balance between efficiency and expressiveness.

2.2 EFFICIENT ATTENTION FOR LONG SEQUENCE MODELING

The Transformer’s quadratic complexity ($O(N^2)$) for self-attention remains a fundamental bottleneck for modeling long sequences. This challenge has driven the recent advances in Large Language Models (LLMs), moving beyond early approximations such as kernelization (Choromanski et al., 2020) or low-rank projections (Wang et al., 2020). More recent breakthroughs include new model classes—State Space Models (e.g., Mamba (Gu & Dao, 2024))—and hardware-aware techniques such as Lightning Attention (Qin et al., 2024) that directly optimize attention computation.

Within recommender systems, progress has often focused on adapting NLP-inspired attention mechanisms to click-through rate (CTR) prediction (Qi et al., 2022; Chen et al., 2022; Song et al., 2025) or using pruning to shorten sequences before attention is applied (Pi et al., 2020). While general-purpose mechanisms for handling set-based inputs exist, they often do not align with the specific needs of sequential recommendation. For instance, the Set Transformer (Lee et al., 2019) and its Pooling Multi-Head Attention (PMA) mechanism efficiently summarize a set into a fixed-size representation using learnable seed vectors. However, their primary goal is permutation-invariant summarization, whereas ranking requires target-aware representations that preserve the sequential nature of user histories.

LIME’s XOR Attention contributes a distinct, task-specific solution. Rather than being a general-purpose approximation of the self-attention matrix, it is a mechanism co-designed with the LIME architecture. By using link embeddings as intermediaries, LIME structurally eliminates the need for direct history-to-history self-attention at inference time. This design enforces a linear complexity ($O(L \cdot N)$) tailored specifically for the user-item ranking context, representing a novel approach to building efficient and expressive sequence models for recommendations.

3 MODEL OVERVIEW

We propose the **Link-based user-item Interaction Modeling for Efficient inference (LIME)**, a novel sequential-modeling architecture tailored for Click-Through Rate (CTR) prediction. LIME is designed to bridge the gap between highly efficient but less expressive two-tower models and powerful but computationally expensive cross-attention architectures. We present its design by progressively building from a simple, efficient baseline to a scalable model with deeper interactions.

To represent a user U ’s interaction history, we learn embedding tables to generate embeddings for each of the $N(U)$ items the user has interacted with. Each item is characterized by a set of attributes, which can be categorical (e.g., user action, topic id) or continuous (e.g., video length), and we learn

embedding tables for each attribute. Continuous features are first transformed into categorical ones via bucketization to index into the embedding tables. For each item, we concatenate the learned embeddings of all its attributes and project them through a Multi-Layer Perceptron (MLP) to obtain a unified representation, E_j . The entire user history is then represented as a sequence of these embeddings, $E = \{E_j\}_{j=1}^{N(U)} \in \mathbb{R}^{N(U) \times d}$.

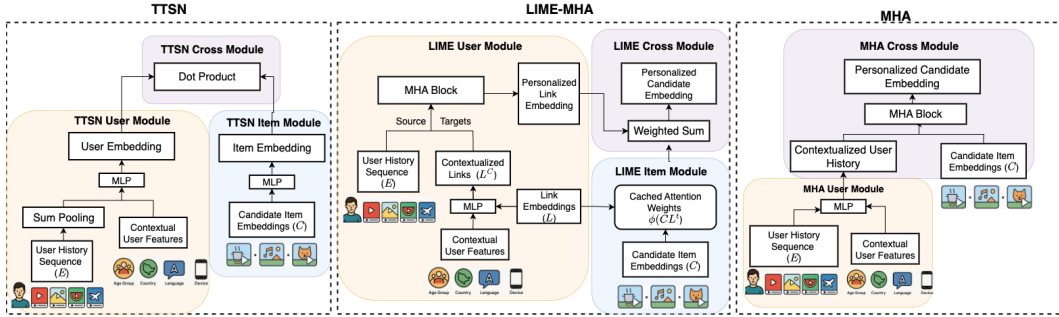


Figure 2: Architecture of TTSN (left), LIME-MHA (middle), and MHA (right). With a lightweight cross module using precomputed attention weights in a decoupled attention framework, LIME-MHA achieves MHA-level expressiveness with similar latency to TTSN.

3.1 FROM TWO-TOWERS TO LIME-MHA: BRIDGING EFFICIENCY AND EXPRESSIVENESS

While a two-tower model (TTSN) is highly efficient for scoring millions of items in retrieval, its expressivity is limited, as user-item interaction is confined to a late-stage dot product. At the other extreme, full cross-attention, prototyped by Multi-Head Attention (MHA), allows deep interaction between every candidate item and the entire user history. However, its computational cost, which scales with both candidate count ($M(U)$) and history length ($N(U)$), places the entire burden on the online interaction stage, making it prohibitively expensive.

LIME-MHA bridges this gap by introducing a small, fixed-size set of $\ell \ll N(U)$ auxiliary tokens, or **link embeddings** $L \in \mathbb{R}^{\ell \times d}$. These learned embeddings act as a compact summary of user interests, which are first personalized based on the user’s history and then exposed to candidate items. This factorization is achieved via two MHA stages, effectively reducing the complexity from $O(M(U) \cdot N(U))$ to $O(\ell(M(U) + N(U)))$.

Multi-Head Attention (MHA), introduced by Vaswani et al. (Vaswani et al., 2017), is a function that maps q query vectors $Q \in \mathbb{R}^{q \times d}$ to outputs using n key and value vectors $K, V \in \mathbb{R}^{n \times d}$ as:

$$\text{MHA}(Q, K, V; M; \theta) = (\phi(\tilde{Q}\tilde{K}^\top) \odot M)\tilde{V} \quad (1)$$

where $\tilde{Q} = QW_Q$, $\tilde{K} = KW_K$, $\tilde{V} = VW_V$, with learnable parameters $\theta = \{W_Q, W_K, W_V \in \mathbb{R}^{d \times d}\}$. Here, ϕ is an activation function (e.g., scaled Softmax or SiLU) and $M \in \{0, 1\}^{q \times n}$ is a binary mask. For instance, $J[i, j] := 1$ is the trivially all-1 mask pattern. $(A \odot B)_{ij} := A_{ij}B_{ij}$ stands for Hadamard product (elementwise multiplication).

The LIME-MHA architecture operates in two steps:

1. User-Side Link Personalization. The globally shared link embeddings L are first contextualized with user features E^C (e.g., location, device type) via an MLP:

$$L^C = \text{MLP}(L \oplus E^C) \quad (2)$$

These contextualized links are then personalized by attending to the user’s full interaction history E using a single MHA layer, producing personalized link embeddings L^P :

$$L^P = \text{MHA}(L^C, E, E; J; \theta) \quad (3)$$

2. Candidate-Side Decoupled Interaction. A key innovation of LIME is how candidate (target) embeddings T interact with the personalized links. Instead of a standard MHA where keys and values both come from L^P , we use the raw, user-independent link embeddings L as keys:

$$O = \text{MHA}(T, L, L^P; J; \theta) = \phi(TL^t)L^P \quad (4)$$

This seemingly small change has a profound impact on efficiency. The attention weight matrix, $\phi(TL^t) \in \mathbb{R}^{M(U) \times \ell}$, is now independent of the user. It can be pre-computed offline for all items in the corpus and cached. At inference time, this expensive matrix multiplication is replaced by a simple lookup, and the interaction reduces to a lightweight weighted sum of the personalized link embeddings L^P . This makes the serving latency per candidate effectively constant, $O(1)$, rather than scaling with history length.

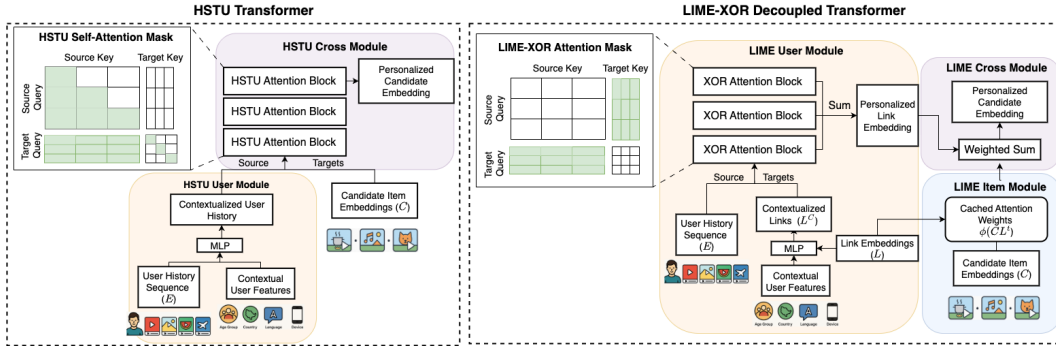


Figure 3: Architecture of HSTU Transformer (left) and LIME-XOR Decoupled Transformer (right) with a visual comparison of our proposed XOR attention mask against the standard HSTU causal self-attention mask.

3.2 FROM LIME-MHA TO LIME-XOR: SCALING TO DEEPER INTERACTIONS

To enhance LIME’s expressiveness, we can deepen the user-side module by stacking multiple interaction layers, akin to the architecture of a multi-layer Transformer. This computation is performed only once per user request, so its complexity does not impact the per-candidate scoring latency. A state-of-the-art approach for this would be to adapt a powerful sequential model block, such as the Hierarchical Sequential Transducer Unit (HSTU) (Zhai et al., 2024), which can be conceptually summarized as follows (see Appendix A for full notations):

$$\text{HSTUBlock}(X; \theta) = \text{GatedMLP}(\text{MHA}(X, X, X; M_{\text{causal}}; \theta); \eta) \quad (5)$$

where $X = E \oplus L^C$ is the concatenation of the user history and contextualized link embeddings. However, the standard HSTU attention uses causal self-attention mask, $M_{\text{causal}}[i, j] := i \geq j$, where every token in the user history attends to all preceding tokens (self-attention) and every candidate attends to the entire user history (cross-attention), results in a computational complexity of $O(N(U)^2 + N(U) \cdot M(U))$. This creates a major bottleneck for users with long interaction sequences or large candidate sets to rank.

To overcome this, we introduce XOR Attention (**XORA**), a novel attention kernel designed to replace the standard self-attention mechanism within the user-side module.

$$\text{XORA}(X, X, X; \theta) = \text{MHA}(X, X, X; M_{\text{xor}}; \theta) \quad (6)$$

$$= \text{MHA}(E, L^C, L^C; J; \theta) \oplus \text{MHA}(L^C, E, E; J; \theta) \quad (7)$$

where $M_{\text{xor}}[i, j] := 1_{i \in [0, |E|]} \wedge 1_{j \in [0, |E|]}$ is the exclusive-or mask pattern that ensures the source and target embeddings attend to one another only. As depicted in Figure 3, the XOR mask structurally eliminates the expensive history-to-history ($E \leftrightarrow E$) interactions. Instead, it facilitates an efficient, two-way, block-wise attention (7): the link embeddings attend to the user history ($L^C \rightarrow E$), and crucially, the user history (source) embeddings also attend back to the link embeddings ($E \rightarrow L^C$).

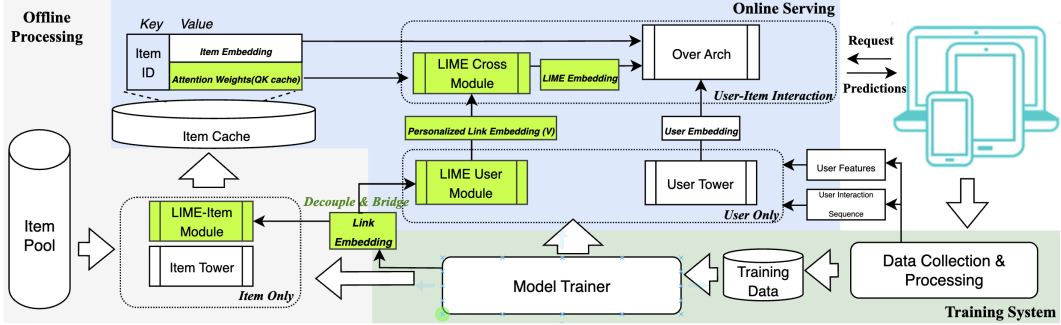


Figure 4: LIME Inference as part of the entire recommendation system

This modification provides two main advantages. First, it reduces the computational complexity from quadratic to linear, $O(\ell \cdot N(U))$, making deep, multi-layer processing of long histories feasible. Second, it enriches the model’s expressivity by enabling the user history representation to be modulated by the global context of the link embeddings from the very first layer.

This leads to our advanced variant, **LIME-XOR**. In this model, we define an **XOR-Layer** by replacing the causal mask in (5) with our efficient XOR mask, M_{XOR} in (6). The personalized links are then computed by stacking and summing the outputs of n such layers:

$$L^P = \sum_{j=1}^n \text{GatedMLP} \left(\text{XORA} \left(E \oplus L^C, E \oplus L^C, E \oplus L^C; \theta \right); \eta_j \right) \quad (8)$$

This entire deep computation occurs on the user side, preserving the efficient, per-candidate scoring mechanism and LIME’s overall scalability. Note that by using contextual links L^C as targets instead of candidate embeddings T , the process remains fully decoupled from individual candidates during this stage.

3.3 LIME’S ARCHITECTURAL ADVANTAGES FOR EFFICIENT INFERENCE

The LIME framework is designed from the ground up to resolve the conflict between model expressiveness and inference latency. Its core efficiency stems from a strategic decoupling of user-side and item-side computations, bridged by the link embeddings. This design enables a multi-stage inference pipeline that maximizes offline pre-computation and minimizes online work, making it highly scalable for real-world recommendation systems.

To facilitate this efficiency, we employ **decoupled attention**, used in the final candidate interaction stage (Equation 4). Instead of using the user-specific personalized links (L^P) for both keys and values, we use the raw, user-independent link embeddings (L) as keys and the personalized links (L^P) as values. This asymmetric structure ensures that the expensive Query-Key dot product, $\phi(CL^t)$, depends only on item-side information (candidate embeddings C and raw links L). Consequently, this attention weight matrix can be pre-computed for all items in the corpus and stored in an efficient key-value store or index, such as FAISS (Johnson et al., 2017), effectively creating a cache of attention weights.

This architectural choice allows us to structure the entire inference process into three distinct stages, as illustrated in Figure 4.

Offline Item-Side Pre-computation. This stage is performed offline whenever the model or item catalog is updated, eliminating redundant computation during online serving. Standard item features are processed by an item tower to produce item embeddings. The decoupled attention weights ($\phi(CL^t)$) between all candidate item embeddings (C) and the raw link embeddings (L) are pre-computed and cached. This transforms the most intensive part of cross-attention into a simple lookup.

Online User-Side Computation. This stage runs once per user request and is independent of the number of candidates being scored. The user’s context and interaction history are processed by the

LIME user module (using either MHA or the multi-layer XOR Transformer) to produce the personalized link embeddings (L^P), as described in Equations (2)–(8). Crucially, this user-side computation can be executed in parallel with the candidate retrieval process. In a production environment, its latency is therefore largely masked, making even a deep, multi-layer Transformer on the user side feasible.

Lightweight User-Item Interaction. This final stage is executed online for each candidate but is extremely lightweight. For each candidate, the pre-computed attention weights are retrieved from the QK Cache. These weights are used to perform a simple weighted sum over the personalized link embeddings (L^P) to generate the final LIME embedding. This embedding is then passed to a shallow interaction network for scoring.

By structuring inference this way, LIME achieves significant computational savings. Compared to a full cross-attention model like HSTU, which has a complexity of $\mathcal{O}(N(U) \cdot (N(U) + M(U)))$, LIME’s complexity is reduced to $\mathcal{O}(\ell \cdot (N(U) + M(U)))$, where $\ell \ll N(U), M(U)$. More importantly, Model serving is reduced to a near-constant time operation with respect to the number of candidates, making LIME highly suitable for latency-sensitive ranking deployments with large candidate sets and long user histories.

4 EXPERIMENTAL RESULTS

4.1 BASELINES, SKYLINES, AND LIME VARIANTS

For baseline we mainly considered **TTSN** (Two-tower sparse network): Depicted in Figure 2, this baseline applies sum-pooling of all the user history embeddings instead of target attention with candidate embeddings.

While we cannot launch naive target attention (candidate against user history) directly for long user histories and large numbers of candidates to rank. But such powerful models can serve as our skyline goal on performance. **MHA Skyline** computes a single layer of target attention between candidate items and user history items. **HSTU Skyline** computes 3 layers of causal self attention and cross attention at each layer, between the candidate items and user history items.

Finally, to thoroughly evaluate our proposed architecture, we conducted experiments with two primary variants of LIME that differ specifically in the sophistication of the link personalization module. **LIME-MHA**: This is the fundamental implementation of our model, as described in Equation (3). It employs a standard attention mechanism to generate a personalized representation for each link by pooling information from the user’s historical item embeddings. **LIME-XOR**: This advanced variant, detailed in Equation (8), incorporates 3-layers of HSTU between the user history and link embeddings for deeper contextualization with our proposed efficient XOR-style masking.

To ensure a fair and controlled comparison, all other architectural components were held constant across all models (see details in Appendix C).

4.2 ACCURACY

We present the normalized entropy metrics as well as (session) AUC metrics for all the variants and baselines/skylines. On the in-house industrial datasets, we measure accuracy on two tasks: video completion (VC) and watch time (WT).

Normalized Entropy (NE) (He et al., 2014) is defined for binary classification task as $NE(\{(p_i, \ell_i)\}_{i=1}^n) := \frac{\sum_{i=1}^n \ell_i \log p_i + (1 - \ell_i) \log(1 - p_i)}{\log(\sum_{i=1}^n \ell_i / n)}$. Note that similar to logloss or binary cross entropy, lower NE means better accuracy. Usually 0.1% drop in NE will lead to online metric improvement.

4.3 INDUSTRIAL EXPERIMENTS SETUP

For the industrial dataset, we take 3 days of logged data for training, and 6 hours for evaluation. Compared to the public datasets, this is a larger scale dataset with longer user history sequences. As shown in Table 5, both LIME variants significantly outperform the TTSN baseline.

Figure 5: Offline, online, and public dataset experimental results.

(a) Industrial Results						(b) Public Dataset Results		
Model	Offline			Online A/B		Model	KuaiRand-1K	Taobao-Ad
	VC	NE	WT	AUC	VC	WT	Click AUC	AUC
TTSN	-	-	-	-	-	-	0.7389 (+0%)	0.6452 (+0%)
LIME-MHA	-0.72%	+0.46%	+28.6%	+22.1%			0.7404 (+0.20%)	0.6468 (+0.25%)
MHA Sky.	-0.73%	+0.53%	N/A	N/A			0.7419 (+0.41%)	0.6462 (+0.15%)
LIME-XOR	-1.04%	+0.76%	+37.9%	+28.6%			0.7351 (-0.51%)	0.6456 (+0.06%)
HSTU Sky.	-1.06%	+0.77%	N/A	N/A			0.7408 (+0.26%)	0.6447(-0.08%)

MHA and HSTU Skylines cannot be tested in online setting due to high serving latency from the large number of candidates.

Model	KuaiRand-1K	Taobao-Ad
TTSN	0.7389 (+0%)	0.6452 (+0%)
DIN	0.7404 (+0.20%)	0.6468 (+0.25%)
SASRec	0.7419 (+0.41%)	0.6462 (+0.15%)
Trunc. MHA	0.7351 (-0.51%)	0.6456 (+0.06%)
LREA	0.7408 (+0.26%)	0.6447(-0.08%)
LIME-MHA	0.7433 (+0.60%)	0.6465 (+0.20%)
MHA Sky.	0.7428 (+0.53%)	0.6464 (+0.19%)
LIME-XOR	0.7448 (+0.80%)	0.6467 (+0.23%)
HSTU Sky.	0.7444 (+0.74%)	0.6475 (+0.36%)

LIME-MHA nearly matches the MHA skyline, while the multi-layer LIME-XOR closes the gap further, achieving performance competitive with the much more complex HSTU skyline across all tasks, even with a 32x sequence compression rate. The 1.04% VC NE improvement of LIME-XOR over the TTSN baseline is a significant gain, which translated to a +37.9% VC and +28.6% WT increase from LIME-ranked candidates during online A/B experiments (Table 5).

For both NLP and CTR prediction tasks, transformer-based models (e.g., LLMs, HSTU) have shown improved performance as compute scales. On our large-scale ranking dataset, the decoupled transformer LIME-XOR similarly achieves substantial gains when scaling sequence length, link count, and model depth. Detailed results are provided in Appendix G.

4.4 PUBLIC EXPERIMENTS SETUP

We also benchmark on public datasets, namely Taobao Ads (Lyu et al., 2020) and KuaiRand-1K dataset (Gao et al., 2022). Taobao-Ads contains 25 million interactions with a maximum sequence length of 50 whereas KuaiRand-1K contains 12 million interactions with a maximum sequence length of 256. To unify data processing and evaluation framework, we leaned heavily on FuxiCTR, a comprehensive sequential recommendation model benchmark platform (Zhu et al., 2020).

On both public datasets, LIME-MHA matches or outperforms the respective skyline with significant improvements over the sum-pooling baseline. The improvement is largest in the KuaiRand-1K dataset as it contains longer sequences (length 256). On KuaiRand-1K, LIME-XOR performs comparably to the HSTU skyline but slightly worse on Taobao-Ad, though still outperforming LIME-MHA models. This is likely due to shorter sequence lengths in Taobao-Ad, leading to noisier results.

We also benchmark existing sequence-compression methods, including Truncated MHA—which applies the MHA skyline only to the most recent ℓ interacted items—and Linformer-style LREA (Song et al., 2025) with a low rank of ℓ . At the same low rank, LIME outperforms both compression techniques. Additionally we benchmark skyline models SASRec (Kang & McAuley, 2018) (a state-of-the-art transformer) and DIN (Deep Interest Network) (Zhou et al., 2018) to validate our LIME variants and skylines are indeed improvements over existing state-of-the-art models.

4.5 ABLATION STUDY

4.6 COMPARISON TO LINEAR ATTENTION METHODS

4.7 INFERENCE SPEED

Figure 1 demonstrates that while MHA and HSTU latency grows significantly with more candidates or longer user histories, LIME’s latency remains nearly constant (see Appendix F for a detailed comparison). This robustness makes it suitable for settings with very long sequences (e.g., >30k items). Furthermore, the user backbone computation can be parallelized with candidate retrieval, masking most of its latency in production and yielding even greater savings.

5 ANALYSIS AND DISCUSSIONS

LIME effectively projects the high-dimensional user-user and user-candidate interaction spaces into low-rank subspaces, acting as a surrogate attention mechanism. This decomposition can be viewed as a structured approximation of the full attention matrix, analogous to techniques in sparse/dense low-rank compression (Figure 7).

To this end, we compute the singular value decomposition (SVD) of the self-attention and cross-attention matrices in a trained HSTU Transformer skyline model averaged across layers and heads over 256 sequence-candidate pairs where each sequence has length 1024 and we rank 1024 candidates against the sequence. In Figure 6, the results clearly demonstrate a long-tailed pattern where the largest 32 singular values (denoted by the vertical black line) capture more than 90% of the information in both self and cross-attention matrices. We also compute the SVD of the raw link embeddings L and personalized link embeddings L^P of a trained LIME-XOR model and analyze the spectral distribution. The singular values of L and L^P demonstrate strong separation amongst the link embeddings with nearly full rank. This analysis indicates that 32 links are able to capture the majority of the information in the self-attention and cross-attention matrices with minimal redundancy for sequence lengths of 1024.

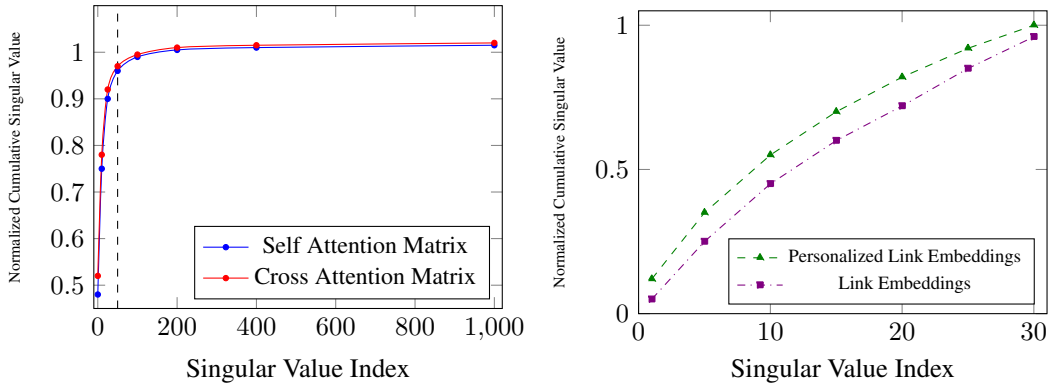


Figure 6: Left: cumulative singular value of self/cross attention matrices in a pretrained transformer model. Right: cumulative singular value of the raw/personalized link embeddings.

6 LIMITATIONS AND FUTURE WORK

Despite LIME’s strong empirical performance, several limitations warrant discussion. First, LIME’s effectiveness relies on the low-rank approximation assumption; domains with highly fragmented user interests may require higher-rank representations. Second, pre-computing QK caches requires periodic updates for evolving item catalogs, which makes it better suited for early stage ranking.

We are actively exploring the following directions: (1) building a larger pool of link embeddings and dynamically selecting link subsets based on user-side features or context, enabling personalized link allocation across different user segments, (2) hierarchical link structures to capture interests at multiple granularities, (3) extensions to multi-modal recommendation and cross-domain transfer learning, and (4) interpretability analysis to understand what semantic patterns individual links capture.

7 CONCLUSION

We proposed LIME, a framework that resolves the efficiency-expressiveness trade-off in large-scale recommenders by using link embeddings as a low-rank approximation for target attention or more general transformer style sequence encoders. Experiments on public and industrial datasets show LIME matches the accuracy of state-of-the-art models like HSTU while drastically reducing inference latency, a result confirmed by significant online A/B test improvements. Our analysis confirmed that LIME’s learned link embeddings effectively capture user interests, validating the low-rank hypothesis. By decoupling the user representation from target items, LIME offers a practical and powerful solution for building high-performance, scalable recommender systems.

8 ACKNOWLEDGEMENT

This work represents the joint work of many engineers, scientists, and leadership supports without whom it will not be possible. We try our best to list them all below in alphabetic order:

Mandy Chen, Siqiao Chen, Bruce Deng, Shilin Ding, Evie Feng, Jerry Fu, Ashish Gandhe, Ning Jiang, Jane Lee, Charlie Li, Han Li, Haotian Li, Rui Li, Zhijing Li, Emma Lin, Xing Liu, Jing Ma, Linjian Ma, Xiaoheng Mao, Franco Mo, Guanyi Mou, Kai Ren, Yongxiong Ren, Yisong Song, Hui Tang, Lingxiao Wang, Meihong Wang, Zhe Wang, Wei Wu, Ye Xu, Jiyan Yang, Wen-Yun Yang, Chenyu Zhao, Liang Zhang, Xinye Zheng, Chao Zhou

REFERENCES

Jianxin Chang, Chenbin Zhang, Zhiyi Fu, Xiaoxue Zang, Lin Guan, Jing Lu, Yiqun Hui, Dewei Leng, Yanan Niu, Yang Song, et al. Twin: Two-stage interest network for lifelong user behavior modeling in ctr prediction at kuaishou. In *Proceedings of the 29th ACM SIGKDD Conference on Knowledge Discovery and Data Mining*, pp. 3785–3794, 2023.

Qiwei Chen, Yue Xu, Changhua Pei, Shanshan Lv, Tao Zhuang, and Junfeng Ge. Efficient long sequential user data modeling for click-through rate prediction. *arXiv preprint arXiv:2209.12212*, 2022.

Krzysztof Choromanski, Valerii Likhoshesterov, David Dohan, Xingyou Song, Andreea Gane, Tamas Sarlos, Peter Hawkins, Jared Davis, Afroz Mohiuddin, Lukasz Kaiser, et al. Rethinking attention with performers. *arXiv preprint arXiv:2009.14794*, 2020.

Paul Covington, Jay Adams, and Emre Sargin. Deep neural networks for youtube recommendations. In *Proceedings of the 10th ACM conference on recommender systems*, pp. 191–198, 2016.

Chongming Gao, Shijun Li, Yuan Zhang, Jiawei Chen, Biao Li, Wenqiang Lei, Peng Jiang, and Xiangnan He. Kuairand: An unbiased sequential recommendation dataset with randomly exposed videos. In *Proceedings of the 31st ACM international conference on information & knowledge management*, pp. 3953–3957, 2022.

Albert Gu and Tri Dao. Mamba: Linear-time sequence modeling with selective state spaces. In *First conference on language modeling*, 2024.

Xinran He, Junfeng Pan, Ou Jin, Tianbing Xu, Bo Liu, Tao Xu, Yanxin Shi, Antoine Atallah, Ralf Herbrich, Stuart Bowers, et al. Practical lessons from predicting clicks on ads at facebook. In *Proceedings of the eighth international workshop on data mining for online advertising*, pp. 1–9, 2014.

Jeff Johnson, Matthijs Douze, and Hervé Jégou. Billion-scale similarity search with gpus, 2017. URL <https://arxiv.org/abs/1702.08734>.

Wang-Cheng Kang and Julian McAuley. Self-attentive sequential recommendation. In *2018 IEEE international conference on data mining (ICDM)*, pp. 197–206. IEEE, 2018.

Juho Lee, Yoonho Lee, Jungtaek Kim, Adam Kosiorek, Seungjin Choi, and Yee Whye Teh. Set transformer: A framework for attention-based permutation-invariant neural networks. In *International conference on machine learning*, pp. 3744–3753. PMLR, 2019.

Xiangyang Li, Bo Chen, HuiFeng Guo, Jingjie Li, Chenxu Zhu, Xiang Long, Sujian Li, Yichao Wang, Wei Guo, Longxia Mao, et al. Inttower: the next generation of two-tower model for pre-ranking system. In *Proceedings of the 31st ACM International Conference on Information & Knowledge Management*, pp. 3292–3301, 2022.

Ze Lyu, Yu Dong, Chengfu Huo, and Weijun Ren. Deep match to rank model for personalized click-through rate prediction. In *Proceedings of the AAAI Conference on Artificial Intelligence*, volume 34, pp. 156–163, 2020.

A Miller. Key-value memory networks for directly reading documents. *arXiv preprint arXiv:1606.03126*, 2016.

Qi Pi, Guorui Zhou, Yujing Zhang, Zhe Wang, Lejian Ren, Ying Fan, Xiaoqiang Zhu, and Kun Gai. Search-based user interest modeling with lifelong sequential behavior data for click-through rate prediction. In *Proceedings of the 29th ACM International Conference on Information & Knowledge Management*, pp. 2685–2692, 2020.

Tao Qi, Fangzhao Wu, Chuhan Wu, and Yongfeng Huang. Fum: Fine-grained and fast user modeling for news recommendation, 2022. URL <https://arxiv.org/abs/2204.04727>.

Zhen Qin, Weigao Sun, Dong Li, Xuyang Shen, Weixuan Sun, and Yiran Zhong. Lightning attention-2: A free lunch for handling unlimited sequence lengths in large language models. *arXiv preprint arXiv:2401.04658*, 2024.

Anshumali Shrivastava and Ping Li. Improved asymmetric locality sensitive hashing (alsh) for maximum inner product search (mips). *arXiv preprint arXiv:1410.5410*, 2014.

Xin Song, Xiaochen Li, Jinxin Hu, Hong Wen, Zulong Chen, Yu Zhang, Xiaoyi Zeng, and Jing Zhang. Lrea: Low-rank efficient attention on modeling long-term user behaviors for ctr prediction. In *Proceedings of the 48th International ACM SIGIR Conference on Research and Development in Information Retrieval*, pp. 2843–2847, 2025.

Ashish Vaswani, Noam Shazeer, Niki Parmar, Jakob Uszkoreit, Llion Jones, Aidan N Gomez, Łukasz Kaiser, and Illia Polosukhin. Attention is all you need. *Advances in neural information processing systems*, 30, 2017.

Sinong Wang, Belinda Z Li, Madian Khabsa, Han Fang, and Hao Ma. Linformer: Self-attention with linear complexity. *arXiv preprint arXiv:2006.04768*, 2020.

Xinyang Yi, Ji Yang, Lichan Hong, Derek Zhiyuan Cheng, Lukasz Heldt, Aditee Kumthekar, Zhe Zhao, Li Wei, and Ed Chi. Sampling-bias-corrected neural modeling for large corpus item recommendations. In *Proceedings of the 13th ACM conference on recommender systems*, pp. 269–277, 2019.

Jiaqi Zhai, Lucy Liao, Xing Liu, Yueming Wang, Rui Li, Xuan Cao, Leon Gao, Zhaojie Gong, Fangda Gu, Michael He, et al. Actions speak louder than words: Trillion-parameter sequential transducers for generative recommendations. *arXiv preprint arXiv:2402.17152*, 2024.

Guorui Zhou, Xiaoqiang Zhu, Chenru Song, Ying Fan, Han Zhu, Xiao Ma, Yanghui Yan, Junqi Jin, Han Li, and Kun Gai. Deep interest network for click-through rate prediction. In *Proceedings of the 24th ACM SIGKDD international conference on knowledge discovery & data mining*, pp. 1059–1068, 2018.

Jieming Zhu, Jinyang Liu, Shuai Yang, Qi Zhang, and Xiuqiang He. Fuxictr: An open benchmark for click-through rate prediction. *CoRR*, 2020.

A SUMMARY OF NOTATIONS

We summarize the key notations used in the paper in Table 1.

B RANKING MODEL ARCHITECTURE COMPARISONS

Outlined in Table 2, two-tower based models have the highest scalability in both candidate set size and user history length but suffer from extremely limited (e.g. dot product) late interaction. Conversely, transformer-based models have deep user-item interactions through full self-attention (amongst user history) and cross-attention (between candidates and user history) at every layer. However, transformer-based models suffer from high latency and low scalability on both user history length and candidate set size.

SIM (Pi et al., 2020) and TWIN (Chang et al., 2023) improve scalability over Transformer-based methods through a two-stage approach. The general-search unit (GSU) first searches for the top- K relevant user history interactions for a particular candidate and exact-search unit (ESU) performs

Symbol	Description
U	User
$N(U)$	Number of items in user U 's interaction history
$M(U)$	Number of candidate items for user U
E_j	Embedding representation of item j
$E = \{E_j\}_{j=1}^{N(U)}$	Sequence of user history embeddings, $E \in \mathbb{R}^{N(U) \times d}$
E^C	User context features (e.g., location, device type)
T	Candidate (target) item embeddings
d	Embedding dimension
$L \in \mathbb{R}^{\ell \times d}$	Link embeddings (auxiliary tokens), $\ell \ll N(U)$
L^C	Contextualized link embeddings (personalized with user features)
L^P	Personalized link embeddings (after attention to user history)
$\text{MHA}(Q, K, V; M; \theta)$	Multi-Head Attention function
W_Q, W_K, W_V	Learnable projection matrices for queries, keys, values ($\in \mathbb{R}^{d \times d}$)
θ, η	Set of learnable parameters
ϕ	Activation function (e.g., scaled Softmax, SiLU)
O	Final LIME output embedding after candidate-side MHA
M	Binary mask for attention, $M \in \{0, 1\}^{q \times n}$
J	All-ones mask pattern, $J[i, j] \equiv 1$
M_{causal}	Causal self-attention mask, $M_{\text{causal}}[i, j] := i \geq j$
M_{xor}	XOR attention mask, $M_{\text{xor}}[i, j] := 1_{i \in [0, E]} \wedge 1_{j \in [0, E]}$
\odot	Hadamard (elementwise) product
\oplus	Concatenation operator
GatedMLP	MLP block with parameters η to learn a gated element-wise product
$\text{HSTUBlock}(X; \theta)$	Hierarchical Sequential Transducer Unit block with parameters θ
XORA	XOR Attention Block
n	Number of stacked XOR layers

Table 1: Notation Table

a full cross-attention against the retrieved items. While the latency is reduced compared to Transformer, we also sacrifice some model expressivity when we completely remove user history self-attention and the GSU runtime complexity is $O(MN)$ which can still be inefficient.

On the other hand, LIME is able to model deep user-item interactions (through the decoupled Transformer framework introduced in Section 3) and achieves high scalability to both candidate set size and user history length when $L \ll N$.

Table 2: Comparison of Ranking Model Architectures where N is the user history length, M is the number of candidates to rank, and $L \ll N$ is the LIME-compressed history size.

Axis	Transformers (HSTU)	SIM/TWIN	Two-Tower	LIME (Ours)
User-Item Interaction	Deep	Medium	Limited late interaction	Deep
Latency	High	Medium	Low	Low
Complexity	$O(MN + N^2)$	$O(MN)$	$O(N)$	$O(ML + NL)$
Pre-computation	Minimal	Minimal	Item Emb	QK Attention Weights

C EXPERIMENT IMPLEMENTATION DETAILS

C.1 DATASET PREPARATION

For the Taobao Ad dataset, we leverage the preprocessed version provided by the FuxiCTR (Zhu et al., 2020) sequential modeling platform. For the KuaiRand dataset (Gao et al., 2022), we pre-process it ourselves by partitioning the first 14 days of interactions for training and last 2 days for testing. We also discarded all items from the train and test set with less than 30 total interactions for

more reliable results. For the industrial dataset, we took 3 days of logged data for model training and 6 hours of data for evaluation.

C.1.1 MODEL HYPERPARAMETERS

For both public datasets and the industrial datasets, we fix model hyperparameters and seeds for all variants for a fair comparison (see Table 3). The industrial dataset is of the largest scale both in terms of the number of interactions and maximum sequence length. Due to the large size of the industrial dataset, we only train for a single epoch in a streaming single-pass setting for the industrial dataset.

Parameter	KuaiRand	TaoBao Ad	Industrial
Num. of Interactions	12×10^6	25×10^6	100×10^9
Learning Rate	1×10^{-4}	1×10^{-3}	4×10^{-4}
Batch Size	1024	8192	1024
Number of Heads	4	4	4
Epochs	2	10	1
Embedding Dimension	32	32	256
Number of Links	16	8	32
Max Sequence Length	256	50	1024
Interaction MLP	[512, 128, 64]	[512, 256, 128]	[96]

Table 3: Model Hyperparameters for KuaiRand, TaoBao Ad, and Industrial datasets

C.2 MODEL DESIGN

Several additional design choices were crucial to stabilize training and ensure generalization:

- **Normalization:** We apply Layer normalization before each linear projection in the QKV projections. Without normalization, the embeddings can drift toward high magnitudes, which can collapse attention weights.
- **Link Initialization:** The raw link embeddings ℓ_i are initialized with samples from a standard normal distribution. This encourages diversity and allows the model to discover interpretable interest clusters during training.
- **Attention Function:** In single-layer MHA experiments we use scaled Softmax which performs the best and in multi-layer transformer experiments we leverage SiLU as the attention activation ϕ .
- **Training Objective:** We use a standard cross-entropy loss with multi-task objectives per request. Other loss terms (e.g., contrastive objectives or auxiliary disentanglement losses) may be explored in future work.

D LOW RANK EXPRESSIONS FOR SELF-ATTENTION AND CROSS-ATTENTION

LIME effectively projects the high-dimensional user-user and user-candidate interaction spaces into low-rank subspaces, acting as a surrogate attention mechanism:

$$\begin{aligned} \text{MHA}(T, E) &\approx \text{MHA}(T, L) \cdot \text{MHA}(L, E), \\ \text{MHA}(E, E) &\approx \text{MHA}(E, L) \cdot \text{MHA}(L, E). \end{aligned}$$

This decomposition can be viewed as a structured approximation of the full attention matrix, analogous to techniques in sparse/dense low-rank compression (e.g. Performer, Linformer, SVDNet).

E INFORMATION BOTTLENECK PERSPECTIVE

From an information-theoretic viewpoint, LIME compresses the user history E into a set of link embeddings L , which are optimized to retain relevance to the user’s behavior (via personalized attention pooling) and retain discriminative power for candidate (T) ranking.

This fits into the Information Bottleneck (IB) principle:

$$\min_L \mathcal{I}(L; E) - \beta \mathcal{I}(L; T)$$

where \mathcal{I} denotes mutual information. That is, we retain only those aspects of the user history that are useful for predicting interaction with candidates.

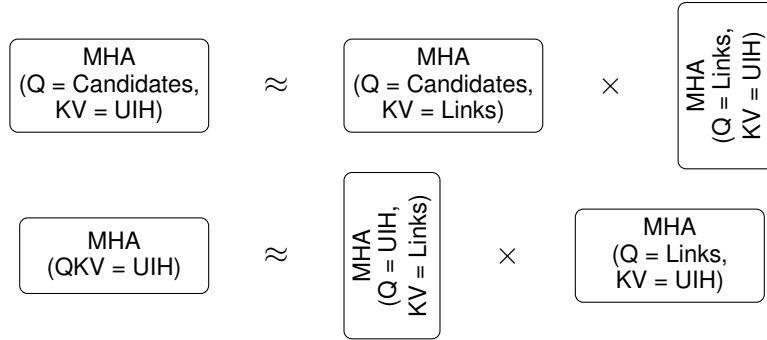


Figure 7: Top: Cross-attention as a low-rank product. Bottom: Self-attention as two low-rank cross-attentions. UIH stands for user interaction history.

F INFERENCE SPEED COMPARISON

Depicted in Figure 1 and Table 4, we observe that LIME-MHA and LIME-XOR have significantly lower latencies under large candidate sets to rank, long user histories, and high QK dimensions (due to the attention weight cacheing).

G SCALING LAW FOR LIME-XOR DECOUPLED TRANSFORMER

Transformers (such as HSTU) have demonstrated strong scaling law for large-scale recommendation systems, mirroring scaling laws from LLMs from NLP. For our decoupled transformer, LIME-XOR, we test scaling across three axes on the large-scale industrial dataset: sequence length, number of links, and number of layers.

From Table 5, we observe that scaling sequence length is very effective in improving both VC NE and WT AUC. However, it is only effective under the presence of sufficient links. Scaling sequence length from 2k to 4k under 32 links is neutral but similar scaling with 256 links demonstrates significant NE and AUC wins. Moreover, for shorter sequences (e.g. 1k) scaling the number of links seems to reach an inflection point faster than scaling links for longer sequences.

From Table 6, we observe that scaling number of layers demonstrates significant NE and AUC improvements which helps demonstrate that LIME-XOR can also achieve scaling law up to the limits we were able to test.

H DERIVATIONS FOR XOR ATTENTION KERNEL

H.1 FORWARD PASS

Let the output of the XOR-attention be $O = (O[S], O[T])$, where S, T stand for source and target respectively. In the context of LIME, source is the user history item embeddings, while target is the link embeddings. Similarly define $Q[S], Q[T], K[S], K[T], V[S], V[T]$ to be the source and target portion of the query, key, value embedding sequences.

$$\begin{aligned} O[T] &= \phi(Q[T]K[S]^\top)V[S] \\ O[S] &= \phi(Q[S]K[T]^\top)V[T] \end{aligned}$$

Table 4: Latency (in seconds) comparison for different models under varying conditions. The columns correspond to the models: LIME-MHA, MHA Skyline, HSTU Skyline, and LIME-XOR. All numerical values are truncated to two decimal places.

(a) vs. Number of Candidates				
# Cand.	LIME-MHA	MHA Sky.	HSTU Sky.	LIME-XOR
16	1.16	0.82	2.59	2.07
32	1.31	0.87	2.64	2.10
64	1.15	0.84	2.59	2.13
128	1.27	0.87	2.52	2.16
256	1.18	0.85	2.62	2.06
512	1.15	0.87	2.63	2.10
1024	1.15	1.06	2.68	2.12
2048	1.13	1.53	2.70	2.07
4096	1.13	1.56	2.93	2.15
8192	1.10	3.40	4.83	2.08
16384	1.15	5.88	7.36	2.06
32768	1.16	9.53	11.77	2.15

(b) vs. User History Length				
Hist. Len.	LIME-MHA	MHA Sky.	HSTU Sky.	LIME-XOR
16	1.13	0.83	1.91	2.71
32	1.14	0.82	1.91	2.11
64	1.15	0.82	1.94	2.08
128	1.13	0.83	2.06	2.03
256	1.10	0.80	1.90	2.03
512	1.11	0.88	1.96	2.10
1024	1.11	1.06	2.27	2.08
2048	1.14	1.55	2.92	2.06
4096	1.14	2.66	7.58	2.11
8192	1.24	3.94	13.65	2.15
16384	1.36	8.55	41.64	2.12

(c) vs. QK Dimension				
QK dim	LIME-MHA	MHA Sky.	HSTU Sky.	LIME-XOR
16	1.22	1.28	7.46	2.56
32	1.28	1.38	7.10	2.55
64	1.25	1.31	7.02	2.57
128	1.26	1.44	7.21	2.59
256	1.26	1.88	8.18	2.65
512	1.24	1.66	7.54	2.64
1024	1.30	3.13	11.02	2.90
2048	1.51	3.31	10.78	3.36
4096	3.07	13.57	35.23	7.93

	32	64	128	256
1k	0%	-0.04%	-0.19%	-0.20%
2k	-0.16%	-0.19%	-0.34%	-0.39%
4k	-0.11%	-0.36%	-0.36%	-0.55%

(a) VC NE % improvement across sequence lengths and link counts

	32	64	128	256
1k	0%	+0.01%	+0.08%	+0.11%
2k	+0.03%	+0.05%	+0.18%	+0.18%
4k	+0.03%	+0.13%	+0.17%	+0.27%

(b) WT AUC across sequence lengths and link counts

Table 5: Performance across varying sequence lengths (1k, 2k, 4k) and link counts (32, 64, 128, 256). Each cell reports metric value and relative change from the baseline (1k, 32 links).

Number of Layers	VC NE % Improvement	WT AUC % Improvement
3	0%	0%
6	-0.25%	+0.12%
9	-0.34%	+0.18%
12	-0.38%	+0.19%

Table 6: VC NE and WT AUC for increasing model depth on fixed 1k sequence length with 32 links.

H.2 BACKWARD PASS

Let $dO[T]$ denote an infinitesimally small change in $O[T]$, also known as the its differential. Similarly define $dO[S]$, $dV[S]$, $dV[T]$, $dQ[S]$, $dQ[T]$, $dK[S]$, $dK[T]$.

Trivially we have

$$\begin{aligned}\frac{\partial O[T]}{\partial Q[S]} &= \frac{\partial O[T]}{\partial K[T]} = \frac{\partial O[T]}{\partial V[T]} = 0 \\ \frac{\partial O[S]}{\partial Q[T]} &= \frac{\partial O[S]}{\partial K[S]} = \frac{\partial O[S]}{\partial V[S]} = 0\end{aligned}$$

The total differential of the loss function is given by

$$dL = \text{Tr} \left(\left(\frac{\partial L}{\partial O[S]} \right)^\top dO[S] \right) + \text{Tr} \left(\left(\frac{\partial L}{\partial O[T]} \right)^\top dO[T] \right).$$

Since $dO[S] = \phi(Q[S]K[T]^\top)dV[T]$ and $dO[T] = \phi(Q[T]K[S]^\top)dV[S]$,

$$dL_V = \text{Tr} \left(\left(\frac{\partial L}{\partial O[S]} \right)^\top \phi(Q[S]K[T]^\top)dV[T] \right) + \text{Tr} \left(\left(\frac{\partial L}{\partial O[T]} \right)^\top \phi(Q[T]K[S]^\top)dV[S] \right).$$

By comparing coefficient with the matrix chain rule $dL_{V[T]} = \text{Tr} \left(\left(\frac{\partial L}{\partial V[T]} \right)^\top dV[T] \right)$, we see that

$$\frac{\partial L}{\partial V[T]} = \phi(K[T]Q[S]^\top) \frac{\partial L}{\partial O[S]}.$$

Similarly

$$\frac{\partial L}{\partial V[S]} = \phi(K[S]Q[T]^\top) \frac{\partial L}{\partial O[T]}.$$

Next for derivatives with respect to Q , we have

$$\begin{aligned} dL_{Q[S]} &= \text{Tr} \left(\left(\frac{\partial L}{\partial O[S]} \right)^\top \phi'(Q[S]K[T]^\top) V[T]K[T]^\top dQ[S] \right) \\ dL_{Q[T]} &= \text{Tr} \left(\left(\frac{\partial L}{\partial O[T]} \right)^\top \phi'(Q[T]K[S]^\top) V[S]K[S]^\top dQ[T] \right). \end{aligned}$$

Hence

$$\begin{aligned} \frac{\partial L}{\partial Q[S]} &= K[T]V[T]^\top \phi'(K[T]Q[S]^\top) \frac{\partial L}{\partial O[S]} \\ \frac{\partial L}{\partial Q[T]} &= K[S]V[S]^\top \phi'(K[S]Q[T]^\top) \frac{\partial L}{\partial O[T]}. \end{aligned}$$

Finally from

$$\begin{aligned} dL_{K[T]} &= \text{Tr} \left(\left(\frac{\partial L}{\partial O[S]} \right)^\top \phi'(Q[S]K[T]^\top) V[T]Q[S]^\top dK[T] \right) \\ dL_{K[S]} &= \text{Tr} \left(\left(\frac{\partial L}{\partial O[T]} \right)^\top \phi'(Q[T]K[S]^\top) V[S]Q[T]^\top dK[S] \right), \end{aligned}$$

we get

$$\begin{aligned} \frac{\partial L}{\partial K[S]} &= Q[T]V[S]^\top \phi'(K[S]Q[T]^\top) \frac{\partial L}{\partial O[T]} \\ \frac{\partial L}{\partial K[T]} &= Q[S]V[T]^\top \phi'(K[T]Q[S]^\top) \frac{\partial L}{\partial O[S]} \end{aligned}$$

I TRITON PSEUDOCODE

Algorithm 1: XOR Mask and Denominator Computation

Require: Query index i , key index j , number of sources n_s

Ensure: Binary mask m , normalization denominator d

```

1: is_srcq  $\leftarrow (i < n_s)$ 
2: is_srck  $\leftarrow (j < n_s)$ 
3:  $m \leftarrow \text{is\_src}_q \oplus \text{is\_src}_k$  ▷ Attend iff exactly one is source
4:  $d \leftarrow \text{is\_src}_q ? n_t : n_s$  ▷ Normalize by opposite partition size return  $m, d$ 

```

Algorithm 2: Forward Pass with Block Range Selection

Require: $\mathbf{Q}, \mathbf{K}, \mathbf{V} \in \mathbb{R}^{n \times d}$, number of sources n_s
Ensure: Output $\mathbf{O} \in \mathbb{R}^{n \times d}$

```

1: for  $q_{\text{start}} \leftarrow 0$  to  $n$  step  $B_M$  do                                 $\triangleright$  Parallel over query blocks
2:    $\mathbf{Q}_b \leftarrow \mathbf{Q}[q_{\text{start}} : q_{\text{start}} + B_M, :]$                        $\triangleright$  Load to SRAM
3:    $\mathbf{acc} \leftarrow \mathbf{0}_{B_M \times d}$ 
4:
5:   // Block range selection (critical optimization)
6:   if  $q_{\text{start}} + B_M \leq n_s$  then                                          $\triangleright$  Pure source queries
7:      $k_{\text{lo}}, k_{\text{hi}} \leftarrow n_s, n$                                           $\triangleright$  Load target keys only
8:   else if  $q_{\text{start}} \geq n_s$  then                                          $\triangleright$  Pure target queries
9:      $k_{\text{lo}}, k_{\text{hi}} \leftarrow 0, n_s$                                           $\triangleright$  Load source keys only
10:  else                                                                $\triangleright$  Boundary case
11:     $k_{\text{lo}}, k_{\text{hi}} \leftarrow 0, n$ 
12:  end if
13:
14:  for  $k_{\text{start}} \leftarrow k_{\text{lo}}$  to  $k_{\text{hi}}$  step  $B_N$  do           $\triangleright$  Over selected K,V blocks
15:     $\mathbf{K}_b \leftarrow \mathbf{K}[:, k_{\text{start}} : k_{\text{start}} + B_N]$                        $\triangleright$  Load K,V to SRAM
16:     $\mathbf{V}_b \leftarrow \mathbf{V}[k_{\text{start}} : k_{\text{start}} + B_N, :]$ 
17:     $\mathbf{S} \leftarrow \mathbf{Q}_b \mathbf{K}_b$                                           $\triangleright$  Compute scores (tensor cores)
18:
19:    for  $i \leftarrow 0$  to  $B_M$  do                                          $\triangleright$  Mask & normalize in registers
20:      for  $j \leftarrow 0$  to  $B_N$  do
21:         $m, d \leftarrow \text{XORMASK}(q_{\text{start}} + i, k_{\text{start}} + j, n_s)$ 
22:         $\mathbf{S}[i, j] \leftarrow m ? \text{SiLU}(\mathbf{S}[i, j]) / d : 0$ 
23:      end for
24:    end for
25:
26:     $\mathbf{acc} \leftarrow \mathbf{acc} + \mathbf{S} \mathbf{V}_b$                                           $\triangleright$  Accumulate (tensor cores)
27:  end for
28:
29:   $\mathbf{O}[q_{\text{start}} : q_{\text{start}} + B_M, :] \leftarrow \mathbf{acc}$                        $\triangleright$  Write to HBM
30: end for
  return  $\mathbf{O}$ 

```

Algorithm 3: Backward Pass (Transposed Access Pattern)

Require: $\mathbf{dO}, \mathbf{Q}, \mathbf{K}, \mathbf{V}$, number of sources n_s
Ensure: Gradients $\mathbf{dQ}, \mathbf{dK}, \mathbf{dV}$

```

1:  $\mathbf{dQ}, \mathbf{dK}, \mathbf{dV} \leftarrow \mathbf{0}$ 
2: for  $k_{\text{start}} \leftarrow 0$  to  $n$  step  $B_N$  do                                 $\triangleright$  Parallel over K,V blocks
3:    $\mathbf{K}_b \leftarrow \mathbf{K}[:, k_{\text{start}} : k_{\text{start}} + B_N]$                           $\triangleright$  Load K,V to SRAM (resident)
4:    $\mathbf{V}_b \leftarrow \mathbf{V}[k_{\text{start}} : k_{\text{start}} + B_N, :]$ 
5:    $\mathbf{dK}_{\text{acc}}, \mathbf{dV}_{\text{acc}} \leftarrow \mathbf{0}_{d \times B_N}, \mathbf{0}_{B_N \times d}$ 
6:
7:   // Symmetric block range selection
8:   if  $k_{\text{start}} + B_N \leq n_s$  then                                          $\triangleright$  Source K,V block
9:      $q_{\text{lo}}, q_{\text{hi}} \leftarrow n_s, n$                                           $\triangleright$  Process target queries only
10:    else if  $k_{\text{start}} \geq n_s$  then                                          $\triangleright$  Target K,V block
11:       $q_{\text{lo}}, q_{\text{hi}} \leftarrow 0, n_s$                                           $\triangleright$  Process source queries only
12:    else                                                                $\triangleright$  Boundary case
13:       $q_{\text{lo}}, q_{\text{hi}} \leftarrow 0, n$ 
14:    end if
15:
16:   for  $q_{\text{start}} \leftarrow q_{\text{lo}}$  to  $q_{\text{hi}}$  step  $B_M$  do                          $\triangleright$  Over selected Q blocks
17:      $\mathbf{Q}_b \leftarrow \mathbf{Q}[q_{\text{start}} : q_{\text{start}} + B_M, :]$ 
18:      $\mathbf{dO}_b \leftarrow \mathbf{dO}[q_{\text{start}} : q_{\text{start}} + B_M, :]$ 
19:      $\mathbf{S} \leftarrow \mathbf{Q}_b \mathbf{K}_b$                                           $\triangleright$  Recompute forward (activation remat)
20:
21:     for  $i \leftarrow 0$  to  $B_M, j \leftarrow 0$  to  $B_N$  do
22:        $m, d \leftarrow \text{XORMASK}(q_{\text{start}} + i, k_{\text{start}} + j, n_s)$ 
23:       if  $m$  then
24:          $s_{ij} \leftarrow \text{SiLU}(\mathbf{S}[i, j]) / d$ 
25:          $\mathbf{S}[i, j] \leftarrow s_{ij} \cdot (1 - s_{ij}) \cdot (1 + \mathbf{S}[i, j]) / d$             $\triangleright$  SiLU gradient
26:       else
27:          $\mathbf{S}[i, j] \leftarrow 0$ 
28:       end if
29:     end for
30:
31:      $\mathbf{dV}_{\text{acc}} \leftarrow \mathbf{dV}_{\text{acc}} + \mathbf{S}^\top \mathbf{dO}_b$                           $\triangleright$  Accumulate (tensor cores)
32:      $\mathbf{dK}_{\text{acc}} \leftarrow \mathbf{dK}_{\text{acc}} + (\mathbf{S}^\top \mathbf{Q}_b)^\top$ 
33:     ATOMICADD( $\mathbf{dQ}[q_{\text{start}} : q_{\text{start}} + B_M, :], (\mathbf{dO}_b \mathbf{V}_b^\top) \mathbf{S}^\top$ )
34:   end for
35:
36:    $\mathbf{dK}[:, k_{\text{start}} : k_{\text{start}} + B_N] \leftarrow \mathbf{dK}_{\text{acc}}$                           $\triangleright$  Write gradients
37:    $\mathbf{dV}[k_{\text{start}} : k_{\text{start}} + B_N, :] \leftarrow \mathbf{dV}_{\text{acc}}$ 
38: end for
return  $\mathbf{dQ}, \mathbf{dK}, \mathbf{dV}$ 

```

J LLM USAGE IN PREPARATION

We used LLM significantly to polish the language of all sections in the paper, including the abstract and appendix sections. The tikz codes in Figure 1, 6 and 7 were generated based on data points we collected ourselves. Most of the tables were also formatted by LLM.